Journal of Magnetism and Magnetic Materials 455 (2018) 39–44

Contents lists available at ScienceDirect

Journal of Magnetism and Magnetic Materials

journal homepage: www.elsevier.com/locate/jmmm

Research articles

Tuning the stability and the skyrmion Hall effect in magnetic skyrmions by adjusting their exchange strengths with magnetic disks

L. Sun [a,b], H.Z. Wu [a], B.F. Miao [a,b], D. Wu [a,b], H.F. Ding [a,b,*]

[a] National Laboratory of Solid State Microstructures and Department of Physics, Nanjing University, 22 Hankou Road, Nanjing 210093, PR China
[b] Collaborative Innovation Center of Advanced Microstructures, Nanjing University, 22 Hankou Road, Nanjing 210093, PR China

ARTICLE INFO

Article history:
Received 20 May 2017
Received in revised form 2 August 2017
Accepted 31 August 2017
Available online 1 September 2017

ABSTRACT

Magnetic skyrmion is a promising candidate for the future information technology due to its small size, topological protection and the ultralow current density needed to displace it. The applications, however, are currently limited by its narrow phase diagram and the skyrmion Hall effect which prevents the skyrmion motion at high speed. In this work, we study the Dzyaloshinskii-Moriya interaction induced magnetic skyrmion that exchange coupled with magnetic nano-disks utilizing the micromagnetic simulation. We find that the stability and the skyrmion Hall effect of the created skyrmion can be tuned effectively with the coupling strength, thus opens the space to optimize the performance of the skyrmion based devices.

The magnetic skyrmion spin structure is a topologically stable state in which the spins point in all directions wrapping into a sphere [1]. Its configuration in a magnetic solid carries a topological charge and Berry phase in real space [2]. Magnetic skyrmions are relatively stable and inert under small perturbations due to the topological protection. And they are also promising candidates for future information technology due to their small size and to the small current densities needed to displace them [3–5]. Also, in contrast to domain walls, the flexibility of skyrmions allows them to be less hindered by defects [3,6,7]. Therefore, magnetic skyrmions have attracted both theoretical and experimental interests due to their unique physical properties and potential applications [3,4,7–26]. Typically, the formation of skyrmion crystal requires the presence of Dzyaloshinskii-Moriya interaction (DMI) and was found to be stable only within a narrow temperature-magnetic field region [2,16,17], which impedes its physical exploration and application. Although major efforts have been made to extend the phase diagram to higher temperatures, it was only recently that DMI-induced room temperature skyrmions were reported [27–31]. In addition, the DMI is commonly weak, which still limits the pool of prospective materials for the skyrmion based applications.

Another interesting phenomenon associated with skyrmion is the skyrmion Hall effect [3,32]. When skyrmion is driven by a spin-polarized current, it does not only move forward but also rotates because of its specific magnetic configuration. Like the Hall effect, a transverse movement, besides the longitudinal motion is generated [33]. The effect, however, significantly limits the speed of the skyrmion motion as the skyrmion can be driven out of the track when a high current is used, resulting in a loss of information. In other words, the skyrmion Hall effect should be suppressed for a skyrmion-based spintronics device for high speed applications [32].

In previous work, we present a method for creating 2D artificial skyrmion crystals with a combination of perpendicularly magnetized film and nanopatterned arrays of magnetic vortices of the same polarity and circulation. The method is demonstrated with micromagnetic simulations and the computed skyrmion number per unit cell [34]. In experiment, the samples are prepared by embedding lithography-patterned arrays of micron-size Co disks onto Co/Pt multilayer films that possess perpendicular magnetic anisotropy. Kerr microscopy imaging and magnetic force microscopy (MFM) demonstrate that the Co disks are in the vortex state where the circulation can be tuned. The measured hysteresis loops are quite similar to those obtained via micromagnetic simulations, revealing the sample can be configured into either skyrmion (skyrmion number $S = \pm 1$) or non-skyrmion ($S = 0$) states [35]. The created skyrmion crystal can be stabilized in a wide temperature and field range, even at room temperature, zero magnetic field, and in the absence of the DM interaction. The created artificial skyrmion crystal can also, reproduce similar eigen modes of the skyrmion crystal due to DMI, evidencing that the intrinsic origin of the dynamics of skyrmion crystal is the nontrivial magnetic texture

* Corresponding author at: National Laboratory of Solid State Microstructures and Department of Physics, Nanjing University, 22 Hankou Road, Nanjing 210093, PR China.
E-mail address: hfding@nju.edu.cn (H.F. Ding).

http://dx.doi.org/10.1016/j.jmmm.2017.08.095
0304-8853/

instead of DMI [36]. Therefore, artificial magnetic skyrmion crystal has both statically and dynamically similar feature with that of skyrmion from DMI. It also possesses much higher stability and tunable skyrmion number. Artificial skyrmion, however, is strongly pinned by geometric constriction, making it unsuitable for skyrmion based racetrack memory [4,37] and logic device applications [38].

The conventional DMI-induced skyrmion has an ultralow current density threshold albeit is only stable within a narrow magnetic field and temperature region. On the other hand, artificial skyrmion has an extended phase diagram, however, loses the mobility. It would be promising for skyrmion-based application if we can combine the advantages of the both type of skyrmions. In our previous work, we present a special magnetic skyrmion, which is based on the advantages of both natural and artificial skyrmion materials. We stack the natural skyrmion crystals and arrays of vortices on each other in close proximity. This leads to increase in stability and suppress of the skyrmion Hall effect due to the attraction of the skyrmion by the disks, but the skyrmion mobility is still compromised. This obstacle can be overcome by decoupling the two original materials from direct coupling to RKKY-type via inserting a spacer with suitable thickness. We find the skyrmion mobility is significantly increased and the stability for the system is enhanced too. With proper tuning of the exchange coupling between the film and the disks, the skyrmion crystal beneath can be moved by a spin-polarized current. Thus, the skyrmion crystal benefit from both the advantages of the natural DMI-induced skyrmion and the artificial skyrmion. The concept is demonstrated as the hybrid magnetic skyrmion in FeGe system [39]. From the application point of view, one needs to optimize the device to obtain the critical parameters such as the moving speed and critical current density *etc*. Therefore, in this work, we present a more detailed study of the properties of the hybrid magnetic skyrmion with different RRKY coupling strengths. This work also serves as a guide for optimizing the parameters for the device design. In addition, we also prove the validation of hybrid skyrmion in a different system, i.e. FeCoSi.

The micromagnetic simulations are performed via the OOMMF code including a bulk-type DMI [40] and the thermal fluctuations [41]. For the calculation of temperature- and field-dependent

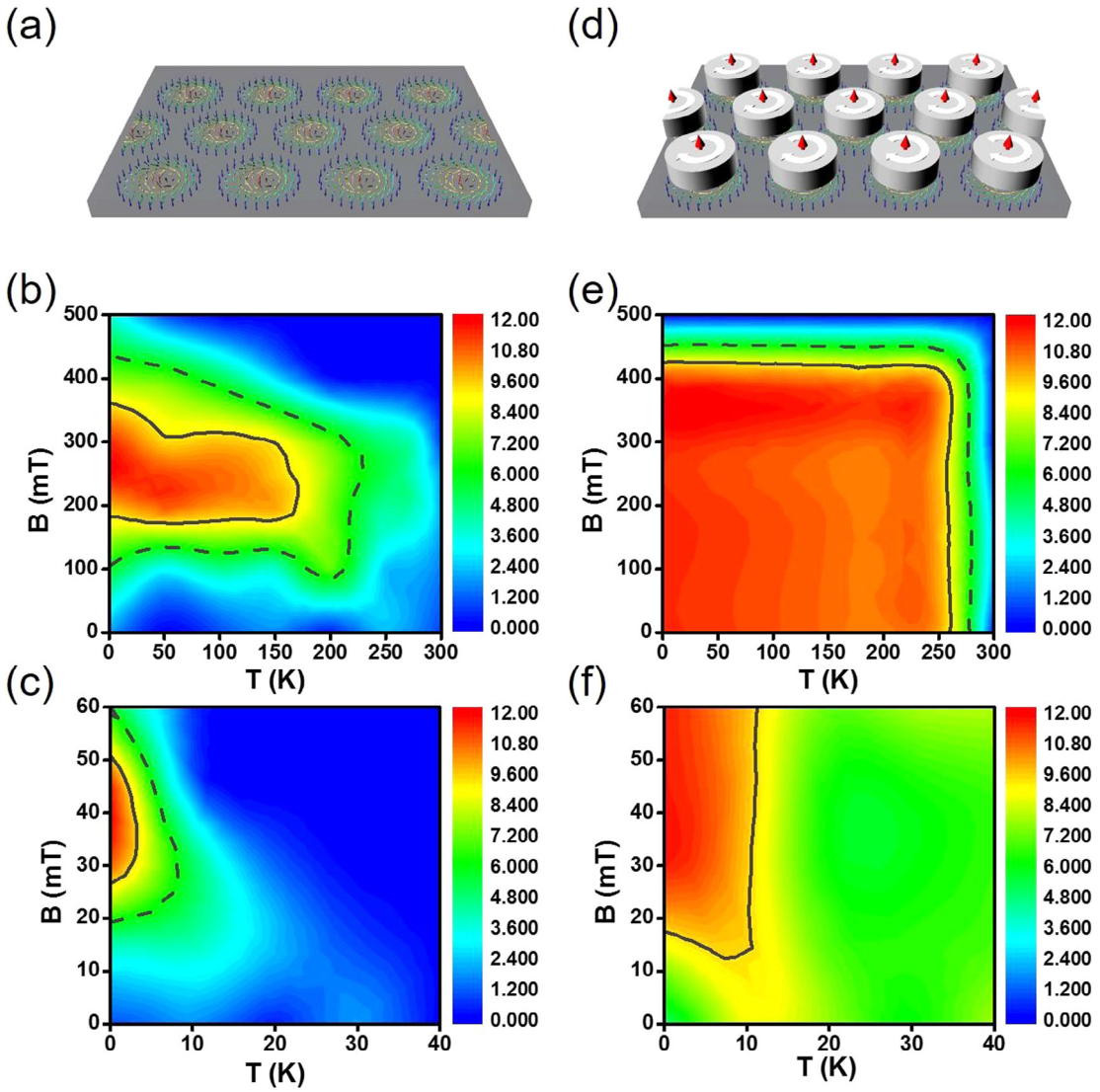

Fig. 1. (a) Schematic of a skyrmion crystal with DMI only, i.e., without Co disk capping. Temperature- and field-dependence of *S* in the 1-nm FeGe thin film (b) and 1-nm FeCoSi thin film (c) without capping vortices. (d) Schematic of a skyrmion crystal with Co disk capping. Temperature- and field-dependence of S in the 1-nm FeGe thin film (e) and 1-nm FeCoSi thin film (f) with Co disk capping. The stability is greatly enhanced in the latter case. The direct exchange coupling strengths between capping vortices and DMI materials are $A_{intra}^{FeGe} = 1.37 \times 10^{-11}$ J/m and $A_{intra}^{FeCoSi} = 3.5 \times 10^{-12}$ J/m. Solid/dash lines in all figures represent isolines with topological number of 80% and 50% of the maximum value, respectively. In (f), the 50%-isolines is beyond the presented region and therefore not shown up.

stability, the dimensions of the magnetic substrate with DMI are chosen to be $210 \times 240 \times 1\ \text{nm}^3$ with the cell size of $2 \times 2 \times 1\ \text{nm}^3$. Material parameters are used for FeGe and FeCoSi in the calculations as follows: experimentally reported temperature dependent saturation magnetization with $M_{sub}^{FeGe} = 3.3 \times 10^5$ A/m and $M_{sub}^{FeCoSi} = 6.0 \times 10^4$ A/m at 0 K [42,43]. The exchange constant $A_{sub}^{FeGe} = 7.54 \times 10^{-12}$ J/m and $A_{sub}^{FeCoSi} = 1.58 \times 10^{-13}$ J/m, is calculated from Curie temperature. Similar approach has been used in Ref. [44]. The DMI constant of FeGe $D^{FeGe} = 1.35\ \text{mJ/m}^2$ is determined from the helical period of 70 nm [45]. Similarly, that of FeCoSi $D^{FeCoSi} = 0.022\ \text{mJ/m}^2$ is determined from the helical period of 90 nm [20,44]. We also include a perpendicular magneto-crystalline anisotropy $K_u^{FeGe} = 1.5 \times 10^5$ J/m^3 and $K_u^{FeCoSi} = 1.2 \times 10^3$ J/m^3, respectively. The magnetic anisotropy may originate from the surface anisotropy and/or the magneto elastic anisotropy caused by the lattice mismatch *etc.* In the calculations for the skyrmion crystal, an array of vortex disks with 60-nm diameter, 70-nm disk spacing for FeGe and 90-nm disk spacing for FeCoSi, and 4-nm thickness are patterned onto the DMI material. The saturation magnetization and exchange constant are $M_{disk} = 1.4 \times 10^6$ A/m and $A_{disk} = 2.5 \times 10^{-11}$ J/m (corresponding to the values of Co), respectively. The coupling between the disks and DMI substrate changes depending on the geometry (see below).

For simulations of the spin transfer torque with current-in-plane geometry, we consider both adiabatic and non-adiabatic terms in the Landau-Lifshitz-Gilbert equation: $\tau_{\text{adiab.}} = u\mathbf{m} \times (\mathbf{m} \times \frac{\partial \mathbf{m}}{\partial x})$ and $\tau_{\text{non-adiab.}} = \beta u(\mathbf{m} \times \frac{\partial \mathbf{m}}{\partial x})$, where $u = \gamma(\hbar jP/2eM_S)$, x is the direction of the electron velocity, γ is the gyromagnetic ratio, M_S is the saturation magnetization, j is the current density, P is the spin polarization, and β is the non-adiabatic damping coefficient [46,47]. In the simulation, the Gilbert damping coefficient α is set to be 0.05, and the non-adiabatic damping β is set to be 0.08. Current flows only within the film with DMI. For the simulation of the nucleation of skyrmions with vertically injected spin polarized current, we consider the in-plane torque $\tau_{IP} = \frac{u}{t}\mathbf{m} \times (\mathbf{m}_P \times \mathbf{m})$, where $\mathbf{m}_p$ is the current polarization vector, and t is the film thickness. In the calculation, the out-of-plane field-like torque is set to be zero.

Fig. 1 (a) and (d) present the schematic of skyrmion lattice without and with vortices capping, respectively. In order to make the quantitative comparison on the stability of the skyrmion before and after capping with the magnetic vortices, we compute the integrated skyrmion number $S = \frac{1}{4\pi}\int \mathbf{m} \cdot \left(\frac{\partial \mathbf{m}}{\partial x} \times \frac{\partial \mathbf{m}}{\partial y}\right) dxdy$ [3,16,48]. The temperature- and field dependent-S for a 1-nm FeGe and FeCoSi film (without capping) is summarized in Fig. 1(b) and (c), respectively. The result is similar to that reported by Huang et al. [11], while that of FeCoSi is slightly smaller compared with experimental observations [17,18]. In comparison, the stability for the system after capping with vortices array is greatly enhanced [Fig. 1 (e) and (f)]. Here the couplings between capping vortices and DMI materials are direct exchange coupling with $A_{intra}^{FeGe} = 1.37 \times 10^{-11}$ J/m and $A_{intra}^{FeCoSi} = 3.5 \times 10^{-12}$ J/m. In order to illustrate the effect better, we define two boundaries where the skyrmion number of the given area has 80% (solid line) and 50% (dash line) of the maximum value. Before capping with the magnetic disk, the skyrmion crystal is stable only for 180–350 mT and <180 K with the 80%-boundary definition in FeGe. After capping, the skyrmion phase is stable for 0–420 mT and <260 K in

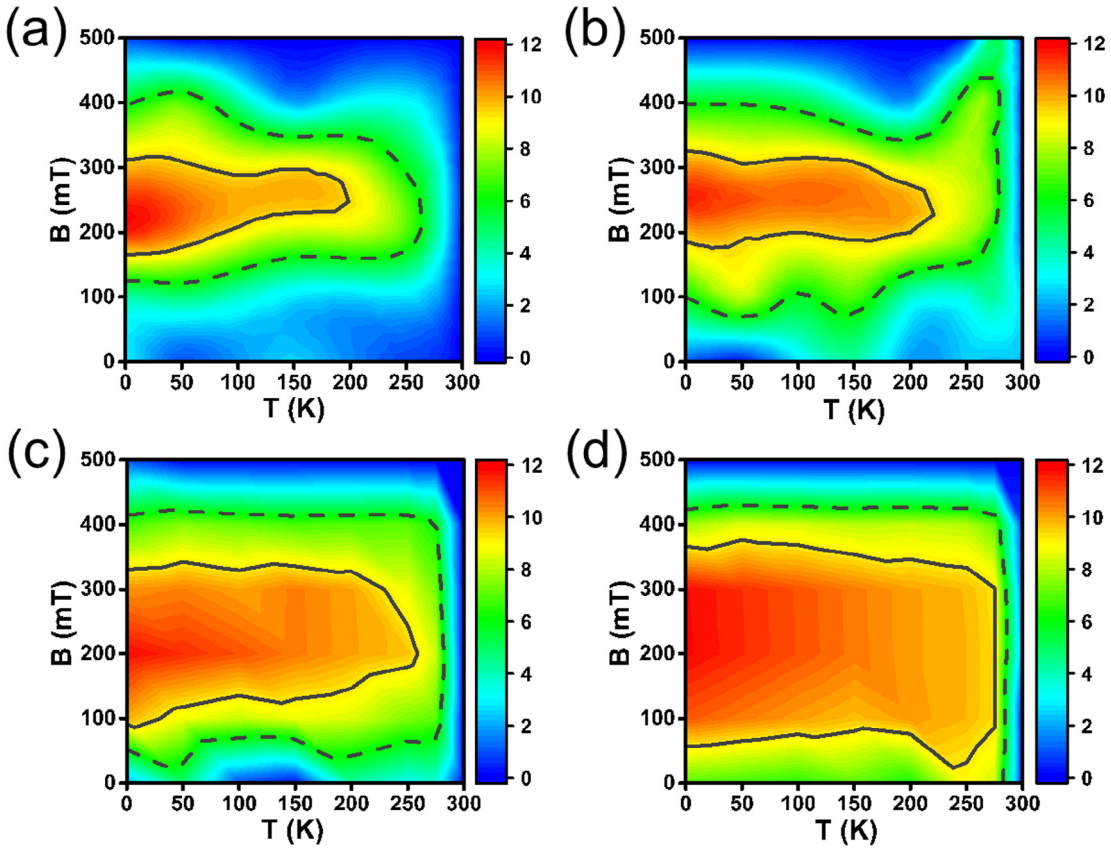

Fig. 2. Temperature- and field-dependence of S in the 1-nm FeGe thin film capped with magnetic vortices, the strength of the RKKY interaction between FeGe and Co vortex is (a) 0.02 mJ/m^2, (b) 0.04 mJ/m^2, (c) 0.08 mJ/m^2 and (d) 0.16 mJ/m^2, respectively.

FeGe, which is significantly larger than that in DMI-only case shown in Fig. 1(b). Similar effect is also found for FeCoSi without and with capping vortices as presented in Fig. 1(c) and Fig. 1(f), respectively. FeCoSi has more limited stability than FeGe, and is stable only for 27–51 mT and <4 K with the 80%-boundary definition due to smaller exchange value and DMI. And skyrmion phase extends to >12 mT and <11 K with capping vortex. Therefore, we demonstrate that the patterning vortex onto the magnetic material with DMI can indeed enhance significantly the stability of the skyrmion crystal beneath.

The stability of skyrmion crystal is increased by capping with the magnetic disk, but the skyrmion mobility is compromised due to strong interlayer coupling. Therefore, we decouple the two original materials from direct coupling to RKKY-type by inserting a spacer with suitable thickness. Fig. 2 shows the temperature- and field-dependent S in FeGe thin film with different RKKY coupling strength, varied from 0.02 mJ/m^2 to 0.16 mJ/m^2 for Fig. 2(a)–(d), respectively. As expected, they clearly demonstrate the stability enhancement of the skyrmion with increasing the RKKY coupling. Even with 0.02 mJ/m^2, the phase diagram for skyrmion has been considerably extended when compared with the natural DMI-induced skyrmion case. When the RKKY coupling strength is 0.16 mJ/m^2, the skyrmion crystal can stable for 60–360 mT and <270 K, which is already similar with that obtained with direct coupling [also see Fig. 1(e)].

With decreasing the RKKY coupling strength, the pining on skyrmion from vortex also decreases. Therefore, the current density threshold is also expected to decrease and the skyrmion can be driven by electrical current with reasonable current density. Fig. 3 presents the comparison of the movement of the skyrmion before and after capping with the magnetic disks. The dimension of the nano-track is $1400 \times 100 \times 1$ nm^3. An in-plane current with density 1.0×10^{13} A/m^2 and spin polarization $P = 0.4$ is injected with electron flow along the nano-track. And the RKKY coupling strength between underlying film with DMI and Co magnetic disks is 0.02 mJ/m^2. To illustrate the one-by-one comparison, we present four groups of snapshots show the position of the skyrmion at different time in Fig. 3. In every group, the upper and lower snapshot correspond to the skyrmion without and with the capping disk respectively. For the skyrmion without capping disk case, the skyrmion can be moved along nano-track with electronic current injected due to the spin transfer torque. In addition to the

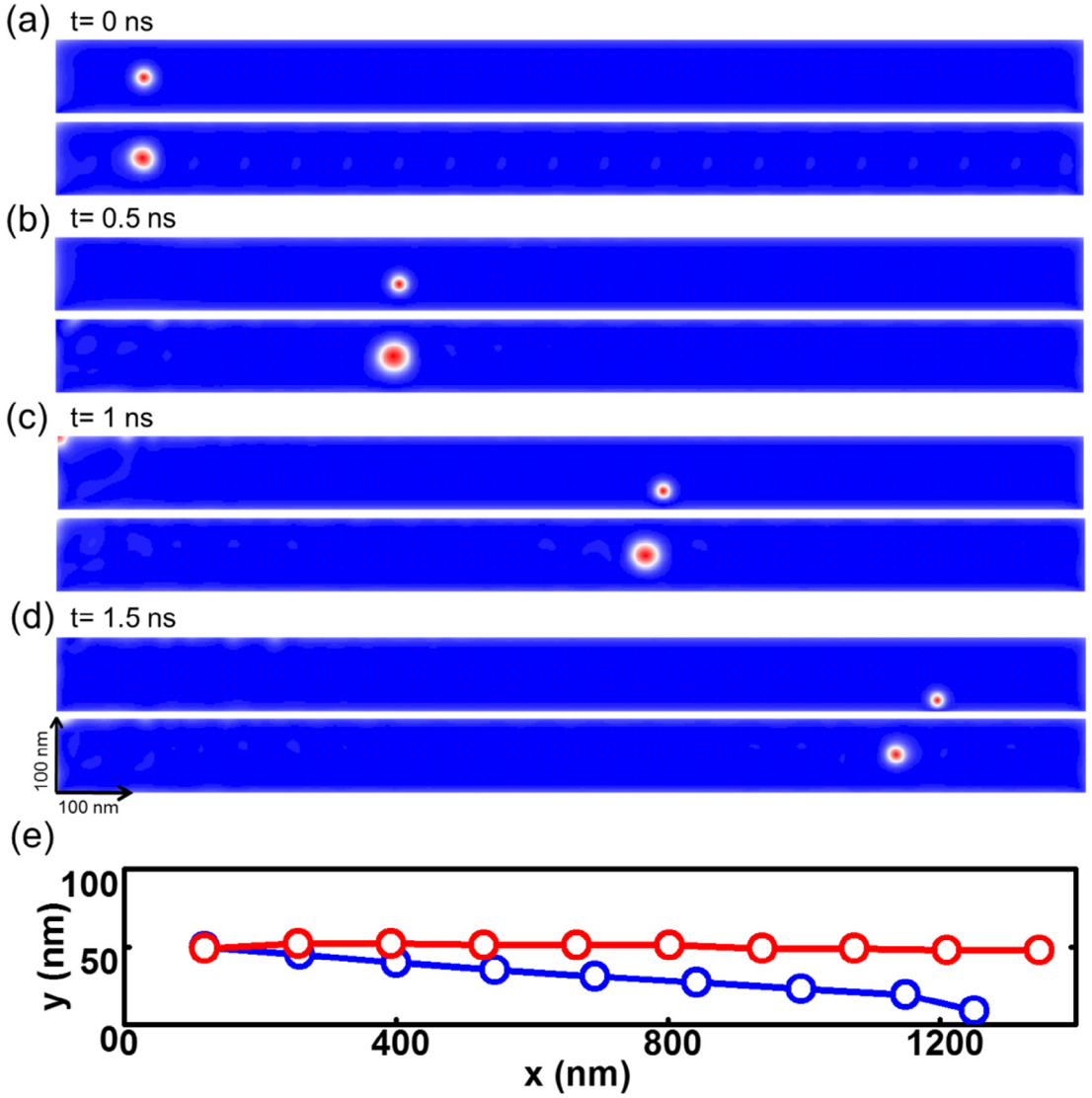

Fig. 3. Snapshots of magnetic configuration (top view) in skyrmion nanotrack at different time sequences. For each point of time, the upper/lower panel represents the case without/with vortex capping, respectively. The RKKY coupling strength between FeGe and Co is 0.02 mJ/m^2. The skyrmion Hall effect is strongly suppressed with vortex capping.

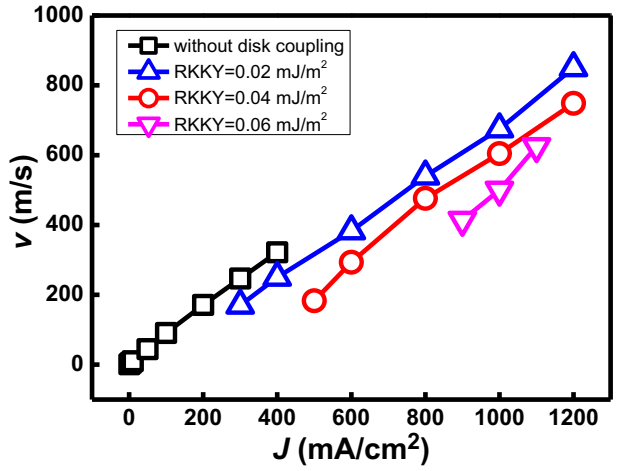

Fig. 4. Skyrmion velocity v as a function of in-plane current density J for skyrmions in DMI film without vortex capping (black square) and with vortex capping and exchanged coupled with different strength. The velocity of skyrmions with DMI only is limited by the skyrmion Hall effect. With increasing the RKKY interaction strength, the current density threshold also increases accordingly.

longitudinal movement, the skyrmion also exhibits a transverse movement, which is the skyrmion Hall effect. If the current density is relatively small, the transverse motion can be balanced by the expelling force from edge and afterwards skyrmion undergoes a steady movement along current direction. Otherwise, the skyrmion would be squeezed out of the nano-track if the current density is too high. As a comparison, we also present the calculated results for the skyrmion exchanged coupled with the magnetic disks. With the same current density, the skyrmion with disk-capping moves a little bit slower than that without capping due to the pining from vortices. And remarkably, we find that the magnetic vortices also act as attracting center and reduce the transverse movement of skyrmion significantly. Fig. 3(e) presents the trajectories for skyrmion without and with capping vortices under current with density of 1.0×10^{13} A/m^2, respectively. The time interval for neighboring position is 0.1 ns. Obviously, the skyrmion Hall effect of skyrmion with capping is strongly suppressed. Thus, the skyrmion with capping in principle can move at higher speed at a higher current density, which is favorable for high speed and high density required for information transfer and storage application.

Fig. 4 shows skyrmion velocity as a function of in-plane current density for skyrmions with DMI only, and that with magnetic disks capped with different RKKY coupling strengths. We find that the current threshold of skyrmions with DMI only is small, well below 1.0×10^{10} A/m^2, and the velocity is linearly proportional to the injected current density. When the current density is over 4.0×10^{10} A/m^2, the skyrmion will deviate from the center of the track and slip away at the edge of the track due to the skyrmion Hall effect, in agreement with previous findings [3,32]. For comparison, we also present the skyrmion velocity as the function of current density with different RKKY coupling strengths. In our simulations, we choose the RKKY coupling strength to be 0.02, 0.04 and 0.06 mJ/m^2, respectively. The velocity of the skyrmion all show an almost linear dependence with a slope similar to that without vortex capping [black square in Fig. 4]. However, the current threshold is increased with the enhancement of RKKY coupling due to the pining effect of the capping magnetic disks. And the skyrmion can move at the speed of more than two times higher of that in natural DMI-induced skyrmion system because of the suppression of the skyrmion Hall effect.

In summary, we demonstrate that by patterning an array of nano-disks onto a magnetic film with DMI, we can combine the high mobility of DMI-induced skyrmion and high stability of artificial skyrmion together. The stability of the skyrmion state can be significantly enhanced due to the coupling from the chiral spins of the vortices above. And the skyrmions beneath can move under the action of a spin-polarized current when the vortices are exchange coupled by a RKKY-type coupling. The capping magnetic disks also act as attracting centers so that the skyrmion Hall effect is effectively suppressed and thus resulting in a higher moving speed. The proposed sandwich structure may also enable the readout of the individual skyrmion via the giant magnetoresistance effect. The stability and speed limit are explored as a function of the exchange coupling strength between the film and the disks and found to be strongly dependent, enabling the possibility in the device optimization.

Acknowledgements

This work was supported by the National Key R&D Program of China (Grant No. 2017YFA0303202); the National Natural Science Foundation of China (Grant Nos. 51571109, 11374145, and 51601087); the Natural Science Foundation of Jiangsu Province, China (Grant No. BK20150565).

References

[1] T.H.R. Skyrme, A unifield field theory of mesons and baryons, Nucl. Phys. 31 (1962) 556–569.
[2] U.K. Roszler, A.N. Bogdanov, C. Pfleiderer, Spontaneous skyrmion ground states in magnetic metals, Nature 442 (2006) 797.
[3] J. Sampaio, V. Cros, S. Rohart, A. Thiaville, A. Fert, Nucleation, stability and current-induced motion of isolated magnetic skyrmions in nanostructures, Nat. Nanotechnol. 8 (2013) 839–844.
[4] A. Fert, V. Cros, J. Sampaio, Skyrmions on the track, Nat. Nanotechnol. 8 (2013) 152–156.
[5] N.S. Kiselev, A.N. Bogdanov, R. Schäfer, U.K. Rößler, Chiral skyrmions in thin magnetic films: new objects for magnetic storage technologies?, J Phys. D: Appl. Phys. 44 (2011) 392001.
[6] J. Iwasaki, M. Mochizuki, N. Nagaosa, Current-induced skyrmion dynamics in constricted geometries, Nat. Nanotechnol. 8 (2013) 742–747.
[7] X.Z. Yu, N. Kanazawa, W.Z. Zhang, T. Nagai, T. Hara, K. Kimoto, Y. Matsui, Y. Onose, Y. Tokura, Skyrmion flow near room temperature in an ultralow current density, Nat. Commun. 3 (2012) 988.
[8] Y. Onose, N. Takeshita, C. Terakura, H. Takagi, Y. Tokura, Doping dependence of transport properties in $Fe_{1-x}Co_xSi$, Phys. Rev. B 72 (2005) 224431.
[9] A. Neubauer, C. Pfleiderer, B. Binz, A. Rosch, R. Ritz, P.G. Niklowitz, P. Böni, Topological Hall effect in the A phase of MnSi, Phys. Rev. Lett. 102 (2009) 186602.
[10] M. Lee, W. Kang, Y. Onose, Y. Tokura, N.P. Ong, Unusual Hall effect anomaly in MnSi under pressure, Phys. Rev. Lett. 102 (2009) 186601.
[11] S.X. Huang, C.L. Chien, Extended skyrmion phase in epitaxial FeGe(111) thin films, Phys. Rev. Lett. 108 (2012) 267201.
[12] O. Petrova, O. Tchernyshyov, Spin waves in a skyrmion crystal, Phys. Rev. B 84 (2011) 214433.
[13] M. Mochizuki, Spin-wave modes and their intense excitation effects in skyrmion crystals, Phys. Rev. Lett. 108 (2012) 017601.
[14] Y. Onose, Y. Okamura, S. Seki, S. Ishiwata, Y. Tokura, Observation of magnetic excitations of skyrmion crystal in a helimagnetic insulator Cu_2OSeO_3, Phys. Rev. Lett. 109 (2012) 037603.
[15] F. Jonietz, S. Muhlbauer, C. Pfleiderer, A. Neubauer, W. Munzer, A. Bauer, T. Adams, R. Georgii, P. Boni, R.A. Duine, K. Everschor, M. Garst, A. Rosch, Spin transfer torques in MnSi at ultralow current densities, Science 330 (2010) 1648–1651.
[16] S. Muhlbauer, B. Binz, F. Jonietz, C. Pfleiderer, A. Rosch, A. Neubauer, R. Georgii, P. Boni, Skyrmion lattice in a chiral magnet, Science 323 (2009) 915–919.
[17] W. Munzer, A. Neubauer, T. Adams, S. Muhlbauer, C. Franz, F. Jonietz, R. Georgii, P. Boni, B. Pedersen, M. Schmidt, A. Rosch, C. Pfleiderer, Skyrmion lattice in the doped semiconductor $Fe_{1-x}Co_xSi$, Phys. Rev. B 81 (2010) 041203.
[18] X.Z. Yu, Y. Onose, N. Kanazawa, J.H. Park, J.H. Han, Y. Matsui, N. Nagaosa, Y. Tokura, Real-space observation of a two-dimensional skyrmion crystal, Nature 465 (2010) 901–904.
[19] X.Z. Yu, N. Kanazawa, Y. Onose, K. Kimoto, W.Z. Zhang, S. Ishiwata, Y. Matsui, Y. Tokura, Near room-temperature formation of a skyrmion crystal in thin-films of the helimagnet FeGe, Nat. Mater. 10 (2011) 106–109.
[20] N. Nagaosa, Y. Tokura, Topological properties and dynamics of magnetic skyrmions, Nat. Nanotechnol. 8 (2013) 899–911.
[21] Y.Y. Dai, H. Wang, P. Tao, T. Yang, W.J. Ren, Z.D. Zhang, Skyrmion ground state and gyration of skyrmions in magnetic nanodisks without the Dzyaloshinsky-Moriya interaction, Phys. Rev. B 88 (2013) 054403.

[22] Y.Y. Dai, H. Wang, T. Yang, W.J. Ren, Z.D. Zhang, Flower-like dynamics of coupled skyrmions with dual resonant modes by a single-frequency microwave magnetic field, Sci. Rep. 4 (2014) 6153.
[23] H.F. Du, R.C. Che, L.Y. Kong, X.B. Zhao, C.M. Jin, C. Wang, J.Y. Yang, W. Ning, R. W. Li, C.Q. Jin, X.H. Chen, J.D. Zang, Y.H. Zhang, M.L. Tian, Edge-mediated skyrmion chain and its collective dynamics in a confined geometry, Nat. Commun. 6 (2015) 78504.
[24] H.F. Du, J.P. DeGrave, F. Xue, D. Liang, W. Ning, J.Y. Yang, M.L. Tian, Y.H. Zhang, S. Jin, Highly stable skyrmion state in helimagnetic MnSi nanowires, Nano Lett. 14 (2014) 2026–2032.
[25] H.F. Du, D. Liang, C.M. Jin, L.Y. Kong, M.J. Stolt, W. Ning, J.Y. Yang, Y. Xing, J. Wang, R.C. Che, J.D. Zang, S. Jin, Y.H. Zhang, M.L. Tian, Electrical probing of field-driven cascading quantized transitions of skyrmion cluster states in MnSi nanowires, Nat. Commun. 6 (2015) 7637.
[26] W. Kang, Y.Q. Huang, X.C. Zhang, Y. Zhou, W.S. Zhao, Skyrmion-electronics: an overview and outlook, Proc. IEEE 104 (2016) 2040–2061.
[27] Y. Tokunaga, X.Z. Yu, J.S. White, H.M. Ronnow, D. Morikawa, Y. Taguchi, Y. Tokura, A new class of chiral materials hosting magnetic skyrmions beyond room temperature, Nat. Commun. 6 (2015) 7638.
[28] G. Chen, A. Mascaraque, A.T. N'Diaye, A.K. Schmid, Room temperature skyrmion ground state stabilized through interlayer exchange coupling, Appl. Phys. Lett. 106 (2015) 242404.
[29] W. Jiang, P. Upadhyaya, W. Zhang, G. Yu, M.B. Jungfleisch, F.Y. Fradin, J.E. Pearson, Y. Tserkovnyak, K.L. Wang, O. Heinonen, S.G.E. te Velthuis, A. Hoffmann, Blowing magnetic skyrmion bubbles, Science 349 (2015) 283–286.
[30] S. Woo, K. Litzius, B. Kruger, M.-Y. Im, L. Caretta, K. Richter, M. Mann, A. Krone, R.M. Reeve, M. Weigand, P. Agrawal, I. Lemesh, M.-A. Mawass, P. Fischer, M. Klaui, G.S.D. Beach, Observation of room-temperature magnetic skyrmions and their current-driven dynamics in ultrathin metallic ferromagnets, Nat. Mater. 15 (2016) 501–506.
[31] C. Moreau-Luchaire, C. Moutafis, N. Reyren, J. Sampaio, C.A.F. Vaz, N. Van Horne, K. Bouzehouane, K. Garcia, C. Deranlot, P. Warnicke, P. Wohlhuter, J.M. George, M. Weigand, J. Raabe, V. Cros, A. Fert, Additive interfacial chiral interaction in multilayers for stabilization of small individual skyrmions at room temperature, Nat. Nanotechnol. 11 (2016) 444–448.
[32] X.C. Zhang, Y. Zhou, M. Ezawa, Magnetic bilayer-skyrmions without skyrmion Hall effect, Nat. Commun. 7 (2016) 10293.
[33] E.H. Hall, On a new action of the magnet on electric currents, Am. J. Math. 2 (1879) 287–292.
[34] L. Sun, R.X. Cao, B.F. Miao, Z. Feng, B. You, D. Wu, W. Zhang, A. Hu, H.F. Ding, Creating an artificial two-dimensional skyrmion crystal by nanopatterning, Phys. Rev. Lett. 110 (2013) 167201.
[35] B.F. Miao, L. Sun, Y.W. Wu, X.D. Tao, X. Xiong, Y. Wen, R.X. Cao, P. Wang, D. Wu, Q.F. Zhan, B. You, J. Du, R.W. Li, H.F. Ding, Experimental realization of two-dimensional artificial skyrmion crystals at room temperature, Phys. Rev. B 90 (2014) 174411.
[36] B.F. Miao, Y. Wen, M. Yan, L. Sun, R.X. Cao, D. Wu, B. You, Z.S. Jiang, H.F. Ding, Micromagnetic study of excitation modes of an artificial skyrmion crystal, Appl. Phys. Lett. 107 (2015) 222402.
[37] X.C. Zhang, G.P. Zhao, H. Fangohr, J.P. Liu, W.X. Xia, J. Xia, F.J. Morvan, Skyrmion-skyrmion and skyrmion-edge repulsions in skyrmion-based racetrack memory, Sci. Rep. 5 (2015) 7643.
[38] X.C. Zhang, M. Ezawa, Y. Zhou, Magnetic skyrmion logic gates: conversion, duplication and merging of skyrmions, Sci. Rep. 5 (2015) 9400.
[39] H.Z. Wu, B.F. Miao, L. Sun, D. Wu, H.F. Ding, Hybrid magnetic skyrmion, Phys. Rev. B 95 (2017) 174416.
[40] M.J. Donahue, D.G. Porter, OOMMF User's Guide Version 1.0, National Institute of Standards and Technology, Gaithersburg, MD, 1999.
[41] X. Fong, OOMMF Oxs extension module of the spin-transfer torque simulations with thermal fluctuations.
[42] N.A. Porter, J.C. Gartside, C.H. Marrows, Scattering mechanisms in textured FeGe thin films: Magnetoresistance and the anomalous Hall effect, Phys. Rev. B 90 (2014) 024403.
[43] N.A. Porter, G.L. Creeth, C.H. Marrows, Magnetoresistance in polycrystalline and epitaxial $Fe_{1-x}Co_xSi$ thin films, Phys. Rev. B 86 (2012) 064423.
[44] M. Beg, R. Carey, W.W. Wang, D. Cortes-Ortuno, M. Vousden, M.A. Bisotti, M. Albert, D. Chernyshenko, O. Hovorka, R.L. Stamps, H. Fangohr, Ground state search, hysteretic behaviour, and reversal mechanism of skyrmionic textures in confined helimagnetic nanostructures, Sci. Rep. 5 (2015) 17137.
[45] B. Lebech, J. Bernhard, T. Freltoft, Magnetic structures of cubic FeGe studied by small-angle neutron scattering, J. Phys.: Condens. Matter 1 (1989) 6105.
[46] J.H. Ai, B.F. Miao, L. Sun, B. You, A. Hu, H.F. Ding, Current-induced domain wall motion in permalloy nanowires with a rectangular cross-section, J. Appl. Phys. 110 (2011) 093913.
[47] M. Yan, A. Kákay, S. Gliga, R. Hertel, Beating the walker limit with massless domain walls in cylindrical nanowires, Phys. Rev. Lett. 104 (2010) 057201.
[48] B. Binz, A. Vishwanath, Chirality induced anomalous-Hall effect in helical spin crystals, Phys. B: Condens. Matter 403 (2008) 1336–1340.